Bioscience, Biotechnology, and Biochemistry
Publication details, including instructions for authors and subscription information:
http://www.tandfonline.com/loi/tbbb20

Lignans from the stems and leaves of Brandisia hancei and their effects on VEGF-induced vascular permeability and migration of HRECs and DLAV formation in zebrafish

Ik-Soo Lee[a], Young Sook Kim[a], Seung-Hyun Jung[a], Song Yi Yu[a], Joo-Hwan Kim[b], Hang Sun[c] & Jin Sook Kim[a]

[a] KM-Based Herbal Drug Development Group, Herbal Medicine Research Division, Korea Institute of Oriental Medicine, Daejeon, Republic of Korea

[b] Department of Life Science, Gachon University, Seongnam, Republic of Korea

[c] Laboratory of Biodiversity and Biogeography, Kunming Institute of Botany, Chinese Academy of Sciences, Kunming, P.R. China

Published online: 15 Dec 2014.

To cite this article: Ik-Soo Lee, Young Sook Kim, Seung-Hyun Jung, Song Yi Yu, Joo-Hwan Kim, Hang Sun & Jin Sook Kim (2015) Lignans from the stems and leaves of Brandisia hancei and their effects on VEGF-induced vascular permeability and migration of HRECs and DLAV formation in zebrafish, Bioscience, Biotechnology, and Biochemistry, 79:4, 581-586, DOI: 10.1080/09168451.2014.991687

To link to this article: http://dx.doi.org/10.1080/09168451.2014.991687

Bioscience, Biotechnology, and Biochemistry, 2015
Vol. 79, No. 4, 581–586

Lignans from the stems and leaves of *Brandisia hancei* and their effects on VEGF-induced vascular permeability and migration of HRECs and DLAV formation in zebrafish

Ik-Soo Lee[1], Young Sook Kim[1], Seung-Hyun Jung[1], Song Yi Yu[1], Joo-Hwan Kim[2], Hang Sun[3] and Jin Sook Kim[1,*]

[1]*KM-Based Herbal Drug Development Group, Herbal Medicine Research Division, Korea Institute of Oriental Medicine, Daejeon, Republic of Korea;* [2]*Department of Life Science, Gachon University, Seongnam, Republic of Korea;* [3]*Laboratory of Biodiversity and Biogeography, Kunming Institute of Botany, Chinese Academy of Sciences, Kunming, P.R. China*

Received September 16, 2014; accepted November 16, 2014
http://dx.doi.org/10.1080/09168451.2014.991687

In our continuing search for novel antiangiogenic agents, a new lignan glycoside, (7*R*,8*R*)-1-(4-*O*-β-D-glucopyranosyl-3-methoxyphenyl)-2-{2-methoxy-4-[1-(*E*)-propene-3-ol]-phenoxyl}-propane-1,3-diol (1), along with three known lignans (2–4), were isolated from the 80% EtOH extract of *Brandisia hancei* stems and leaves. These isolates (1–4) were subjected to an *in vitro* bioassay to evaluate their effects on vascular endothelial growth factor (VEGF)-induced vascular permeability and migration of human retinal endothelial cells (HRECs). Of the compounds tested, compound 1 resulted in the greatest reduction in VEGF-induced vascular permeability by about 31.5% at 10 μM compared to the VEGF-treated control. In the migration assay, compounds 1 and 2 significantly decreased VEGF-induced HREC migration. Furthermore, zebrafish embryos treated with compounds 1 and 2 showed mild reductions of dorsal longitudinal anastomotic vessel (DLAV) formation.

Key words: *Brandisia hancei*; Scrophulariaceae; lignans; vascular endothelial growth factor; zebrafish

Brandisia hancei Hook. f. (Scrophulariaceae), which is primarily distributed throughout southwestern China, has been used in traditional Chinese medicine since ancient times. The whole plant is prescribed to treat chronic and acute osteomyelitis, rheumatoid arthritis, chronic hepatitis, hyperlipemia, and hypercholesterolemia, while the roots and leaves are considered useful in the treatment of hepatitis, hematuria, enterorrhagia, and metritis.[1)] Due to its potential medicinal value, this plant has been the focus of much attention in the search for pharmacologically significant compounds. A number of phenylethanoid glycosides, including acteoside, isoacteoside, 2′-*O*-acetylacteoside, brandioside, arenarioside, and poliumoside, have been characterized from *B. hancei*[1–4)] and reported to exhibit diverse and potentially significant pharmacological activities, including antiproliferative,[4)] antioxidant,[5)] antiinflammatory,[6)] anticancer,[7)] hepatoprotective,[8)] antinephritic,[9)] cardioactive,[10)] and antimicrobial[11)] effects. Flavonoids and iridoid glycosides are also common in the Scrophulariaceae family, but only the flavone, luteolin, and iridoid glycoside, mussaenoside, have been found in *B. hancei*.[3)] Other components reported in this plant are monosaccharides, dulcitol and mannitol, and β-sitosterol glycosides, daucosterol and β-sitosterol gentiobioside.[1–3)] However, some minor constituents of this plant remain to be characterized.

Angiogenesis, the formation of new blood vessels from pre-existing vasculature, is an essential process under both physiological and pathological conditions, such as tumor growth, rheumatoid arthritis, heart disease, atherosclerosis, and various eye diseases.[12)] Angiogenesis is tightly regulated by the balance between production of stimulators and inhibitors. Vascular endothelial growth factor (VEGF), also known as vascular permeability factor (VPF), is a potent angiogenic stimulator with endothelial cell-specific mitogenic activity and exerts a pivotal role in both normal and pathological angiogenesis.[13)] This factor regulates vascular endothelial cell proliferation, migration, invasion, and permeability.[14)] The overexpression of VEGF is associated with chronic inflammation, tumor growth, and other angiogenesis-related diseases.[14)]

In our continuing search for novel antiangiogenic agents from natural sources, we found that the 80% EtOH extract of *B. hancei* stems and leaves exhibited a considerable inhibitory effect on VEGF-induced vascular permeability in human retinal endothelial cells

*Corresponding author. Email: jskim@kiom.re.kr
Abbreviations: BSA, bovine serum albumin; DLAV, dorsal longitudinal anastomotic vessel; HBSS, balanced salt solution; HRECs, human retinal endothelial cells; PBS, phosphate-buffered saline; VEGF, vascular endothelial growth factor.

(HRECs). Further phytochemical study of this plant resulted in the isolation of a new lignan glycoside (**1**), together with three known lignans (**2**–**4**). This report describes the isolation and structural elucidation of these compounds, as well as the characterization of their inhibitory effects on VEGF-induced vascular permeability and migration in HRECs. We further investigated the effects of isolated compounds on DLAV formation *in vivo* in a zebrafish model.

Materials and methods

General experimental procedures. Optical rotations were measured on a JASCO P-2000 digital polarimeter. ^{1}H (300 MHz) and ^{13}C NMR (75 MHz) spectra were obtained using a Bruker DRX-300 spectrometer with TMS as an internal standard. 2D-NMR experiments (COSY, HMQC, HMBC, and NOESY) were run on a Bruker Avance 500 NMR spectrometer. HR-ESI-MS were recorded on a Shimadzu LCMS-IT-TOF spectrometer. Column chromatography was performed using silica gel (70–230 mesh and 230–400 mesh, Merck), YMC-gel ODS-A (S-75 μm, YMC), and Sephadex LH-20 (Amersham Pharmacia Biotech). Thin-layer chromatography (TLC) was performed on pre-coated silica gel 60 F_{254} (0.25 mm, Merck) and RP-18 F_{254s} plates (0.25 mm, Merck). Spots were detected by UV light (254 nm) and spraying with 10% H_2SO_4 followed by heating.

Plant material. The stems and leaves of *B. hancei* were collected in Songying, Yunnan, China, in October 2008, and identified by Prof. J.-H. Kim, Gachon University, Republic of Korea. A voucher specimen (DiAB-2008-085) has been deposited in the Herbarium of the Diabetic Complications Research Team, Korea Institute of Oriental Medicine, Republic of Korea.

Extraction and isolation. The air-dried stems and leaves of *B. hancei* (3.0 kg) were extracted with 80% aqueous EtOH (each 30 L, three times) at room temperature for 7 days, filtered, and concentrated to give an 80% EtOH extract (332 g). The extract (90 g) was subjected to silica gel column chromatography (70–230 mesh, 100 × 9.5 cm) eluted with a gradient solvent system consisting of $CHCl_3$/MeOH (100:1 → 30:70) to yield 10 fractions [A–J]. Chromatography of fraction D (13.3 g) on a silica gel column (230–400 mesh, 60 × 3.5 cm) eluted with a gradient solvent system of EtOAc/MeOH/H_2O (9:1:0.2 → 8:2:0.5) yielded eight subfractions (D1–D8). Subfraction D4 (0.9 g) was further purified by extensive preparative RP-HPLC [Gilson trilution system; YMC-pack Pro C_{18} (S-5 μm, 250 × 10 mm) column; MeCN/H_2O (12:88); UV detection, 270 nm; flow rate, 4.0 mL/min] to obtain compounds **2** (10 mg) and **3** (8 mg). Fraction D (2.6 g) was further separated on a Sephadex LH-20 column (50 × 2.0 cm) eluted with a MeOH/H_2O gradient (1:1 → 1:0) to generate six subfractions (D1–D6). Compound **4** (7 mg) was isolated from subfraction D2 (0.6 g) using a YMC RP-18 column (46 × 1.8 cm) eluted with a MeOH/H_2O gradient (3:7 → 6:4). Preparative RP-HPLC [Gilson trilution system; YMC-pack Pro C_{18} (S-5 μm, 250 × 10 mm) column; MeCN/H_2O (15:85); UV detection, 270 nm; flow rate, 4.0 mL/min] of subfraction D5 (0.6 g) obtained compound **1** (4 mg).

(7R,8R)-1-(4-O-β-D-glucopyranosyl-3-methoxyphenyl)-2-{2-methoxy-4-[1-(E)-propene-3-ol]-phenoxyl}-propane-1,3-diol (1): white powder; [α]\[25D\] −23.0° (*c* 0.1, MeOH); UV λ_{max} (MeOH) 230, 272 nm; CD (MeOH) Δε (nm) −10.4 (228), −4.8 (245); ^{1}H and ^{13}C NMR, see Table 1; HR-ESI-MS *m/z* 561.1943 $[M + Na]^+$ (Calcd. for $C_{26}H_{34}O_{12}Na^+$: 561.1942).

Acid hydrolysis. Compound **1** (2 mg) in 10% HCl/dioxane (1:1, 1 mL) was heated at 80 °C for 3 h in a water bath. The mixture was neutralized with Ag_2CO_3, filtered, and extracted with EtOAc (20 mL). The aqueous layer was evaporated, and the residue was treated with L-cysteine methyl ester hydrochloride (2 mg) in pyridine (0.5 mL) at 60 °C for 1 h. After the reaction was completed, the solution was treated with Ac_2O (3 mL) at 60 °C for 1 h. Authentic samples were prepared by the same procedure. The acetate derivatives were subjected to gas chromatography (GC) analysis under the following conditions: GC-2010 (Shimadzu, Kyoto, Japan) instrument; detector, FID; column, TC-1 capillary column (0.25 mm × 30 cm; GL Science, Tokyo, Japan); column temperature, 230 °C; programmed increase, 38°C/min; carrier gas, N_2 (1 mL/min); injection and detector temperature, 270 °C. The sugar derivative thus obtained showed a retention time of 21.10 min, identical to that of authentic D-glucose.

Table 1. ^{1}H (300 MHz) and ^{13}C NMR (75 MHz) and HMBC data for compound 1 (in CD_3OD).

Position	^{1}H (*J* in Hz)	^{13}C	HMBC (H → C)
1		138.2	
2	7.10 d (1.5)	113.1	1, 3, 4, 6, 7
3		150.9	
4		147.8	
5	7.08 d (8.0)	118.1	1, 3, 4, 6
6	6.94 dd (8.0, 1.5)	121.5	2, 4, 5, 7
7	4.86 d (6.4)	74.3	1, 2, 6, 8, 9
8	4.38 ddd (6.4, 5.5, 4.0)	86.3	1, 7, 9, 3′
9	3.87 dd (11.8, 5.5), 3.76 dd (11.8, 4.0)	62.6	7, 8
3-OMe	3.81 s	57.1	3
1′		133.4	
2′	6.98 d (1.2)	111.7	1′, 3′, 4′, 6′, 7′
3′		149.2	
4′		152.3	
5′	6.85 d (7.8)	119.0	1′, 3′, 4′, 6′
6′	6.86 dd (7.8, 1.2)	121.1	1′, 5′, 7′
7′	6.50 brd (15.5)	131.9	1′, 6′, 8′
8′	6.23 dt (15.5, 5.5)	129.1	1′, 6′, 7′, 9′
9′	4.20 dd (5.5, 1.0)	64.2	7′, 8′
5′-OMe	3.80 s	56.9	5′
1″	4.81 d (7.5)	103.5	4, 2″
2″	3.47 m	75.3	1″, 3″
3″	3.39 m	78.6	2″, 4″
4″	3.39 m	71.8	3″, 5″
5″	3.45 m	78.2	4″, 6″
6″	3.86 m, 3.68 m	62.9	3″, 4″, 5″

Cell culture. HRECs (Cat. No. ACBRI 181) were purchased from Cell Systems (Kirkland, WA) and used at passages 3–7. Cells were grown in CSC complete medium (CS-4ZO-500; Cell Systems) containing Bac-Off (antibiotic). Cultures were maintained as described previously.[15)]

Permeability assay. HRECs were plated at 2×10^5 cells/mL on Transwell inserts and cultured for 72 h in growth medium. Following this culture period, cells were treated with VEGF (20 ng/mL) and **1**–**4** (each 10 μM). After treatment, the inserts were washed with Hank's balanced salt solution (HBSS), and FITC-dextran (ECM644; Millipore, Bedford, MA) was added to the top chamber. After 24 h, samples were removed from the bottom chamber and read in a microplate fluorometer (Synergy HT; Biotek, Winooski, VT) at an excitation wavelength of 485 nm and emission wavelength of 535 nm. Experiments were performed in triplicate.

Wound-healing cell migration assay. HRECs were plated at 1×10^5 cells/well on 12-well plates in normal culture medium and allowed to reach 80–90% confluence. Migration assay was performed as described previously.[15)] A wound with a width of 0.6–1 mm was made with a sterile pipette tip, and cells were rinsed with phosphate-buffered saline (PBS). Fresh culture medium containing VEGF was added to the wells, and the cells were incubated for 6 h. To determine the inhibitory effects of **1**–**4** on migration, cells were pretreated with depletion medium containing 0.5% bovine serum albumin (BSA) with or without **1**–**4** (each 10 μM). Cell migration was monitored by visual examination using an inverted microscope (BX51; Olympus, Tokyo, Japan). Experiments were performed in triplicate.

Zebrafish and DLAV formation assay. All experimental protocols for animal care and use were approved by the local ethics board (Korea Institute of Oriental Medicine Animal Care and Use Committee), and animal husbandry and procedures were performed according to institutional guidelines. Adult zebrafish were maintained under standard conditions at 28.5 °C with a 14-h light/10-h dark cycle. Embryos were obtained from crosses between *flk*:EGFP transgenic zebrafish and raised in egg water (sea salt, 0.06 g/L). For DLAV formation assays, *flk*:EGFP zebrafish embryos were distributed into 24-well microplates (8–10 embryos per well) and treated with compounds **1**–**4** (each 80 μM) and VEGF receptor tyrosine kinase inhibitor at 1 μM (Cat. No. 676500; Calbiochem, Darmstadt, Germany). The embryos were incubated for 11 h postfertilization (hpf) and observed for gross morphological changes using a confocal microscope (FV10i; Olympus) and a stereomicroscope (SZX16; Olympus) at 29 hpf. Experiments were performed in triplicate.

Statistical analysis. The results are expressed as means ± standard error of the mean (SEM) from multiple experiments. Statistical significance was assessed using one-way analysis of variance (ANOVA) and Dunnett's multiple comparison tests with the GraphPad 5.0 Prism software (GraphPad, San Diego, CA, USA).

Results and discussion

The 80% EtOH extract of *B. hancei* stems and leaves, which significantly inhibited VEGF-induced vascular permeability in HRECs, was subjected to a series of chromatographic techniques, leading to the isolation of a new lignan glycoside (**1**) and three known lignans (**2**–**4**) (Fig. 1). By comparing their physicochemical and spectral data with those in the literature, three compounds were identified: (–)-5′-methoxyisolariciresinol 3α-*O*-β-D-glucopyranoside (**2**),[16)] lyoniresinol 3α-*O*-β-D-glucopyranoside (**3**),[16)] and isolariciresinol 3α-*O*-β-D-glucopyranoside (**4**).[16)]

Compound **1** was obtained as a white amorphous powder with negative specific rotation, [α]\[25D\] − 23.0° (*c* 0.1, MeOH). High-resolution ESI-MS analysis of **1** yielded a molecular ion peak at *m/z* 561.1943 $[M + Na]^+$, in accordance with the molecular formula $C_{26}H_{34}O_{12}$. The UV absorption maxima of **1** in MeOH at 230 and 272 nm suggested the presence of aromatic ring(s). Acid hydrolysis of **1** yielded an aglycone and a monosaccharide unit. The ^{1}H NMR spectrum of the aglycone unit showed six aromatic protons as two ABX systems, one at δ_H 7.10 (1H, d, J = 1.5 Hz), 7.08 (1H, d, J = 8.0 Hz), and 6.94 (1H, dd, J = 8.0, 1.5 Hz), and another at δ_H 6.98 (1H, d, J = 1.2 Hz), 6.86 (1H, dd, J = 7.8, 1.2 Hz), and 6.85 (1H, d, J = 7.8 Hz) (Table 1), which suggested the presence of two 1,3,4-trisubstituted benzene rings. In addition, the aglycone unit showed the ^{1}H NMR signals for two oxygenated methines [δ_H 4.86 (1H, d, J = 6.0 Hz) and 4.38 (1H, ddd, J = 6.0, 5.5, 4.0 Hz)], two oxygenated methylenes [δ_H 3.87 (1H, dd, J = 11.8, 5.5 Hz) and 3.76 (1H, dd, J = 11.8, 4.0 Hz) and δ_H 4.20 (2H, dd, J = 5.5, 1.0 Hz), a *trans*-olefin [δ_H 6.50 (1H, brd, J = 15.5 Hz) and 6.23 (1H, dt, J = 15.5, 5.5 Hz)], and two methoxys [δ_H 3.81 and 3.80 (each 3H, s)]. The ^{13}C NMR spectrum (Table 1), combined with the HMQC data, showed that **1** contained 26 carbons, of which 20 carbon signals were assigned to an aglycone unit and 6 to a monosaccharide unit. The six carbon signals at δ_c 103.5, 78.6, 78.2, 75.3, 71.8, and 62.9 and an anomeric proton signal at δ_H 4.81 of **1** were typical of a glycopyranosyl unit, which was identified as D-glucose followed by GC analysis of the acid hydrolysate. Moreover, the large coupling constant (J = 7.5 Hz) of the anomeric proton indicated that the glycopyranosyl unit was linked in a β-configuration. The location of a glycopyranosyl unit at C-4 was elucidated from the HMBC correlation between the anomeric proton signal at δ_H 4.81 (H-1″) and the aglycone carbon signal at δ_c 147.8 (C-4) (Fig. 2). The ^{1}H–^{1}H COSY correlation between the olefinic protons (δ_H 6.50 and 6.23) and the oxygenated methylene protons (δ_H 3.87 and 3.76) suggested the presence of an allyl alcohol moiety in **1** (Fig. 2). The linkage position of this moiety was determined to be the C-1′ position based on the HMBC experiment (Fig. 2 and Table 1). These spectroscopic data were similar to those of citrusin A, an 8-*O*-4′

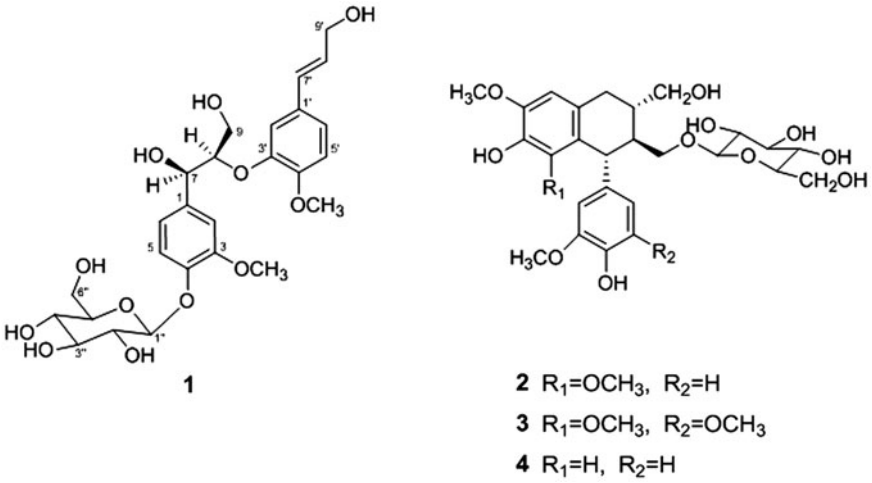

Fig. 1. Chemical structures of compounds **1**–**4** from *B. hancei*.

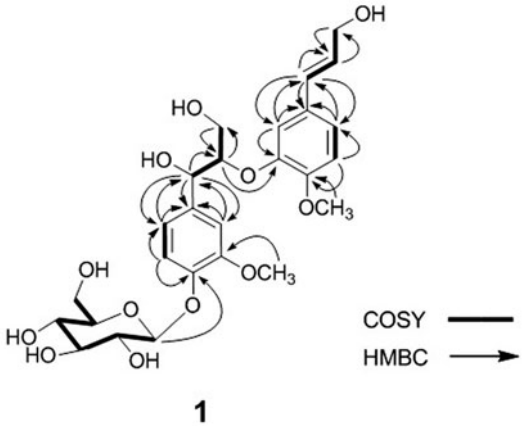

Fig. 2. Key ^{1}H–^{1}H COSY and HMBC correlations for compound **1**.

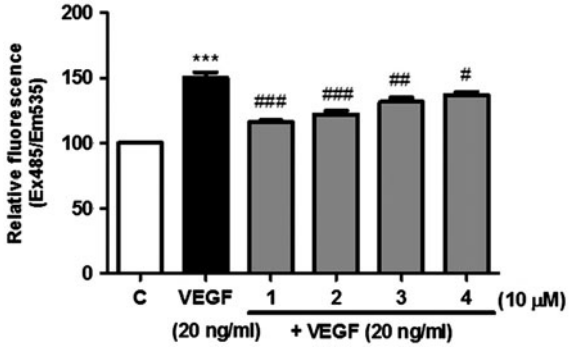

Fig. 3. Inhibitory effects of compounds **1**–**4** from *B. hancei* on VEGF-induced vascular permeability in HRECs.

Notes: HRECs were seeded at 2 × 10^5 cells per insert and cultured for 72 h in growth medium. Following this culture period, cells were treated with VEGF (20 ng/mL) and **1**–**4** (each 10 μM) for 24 h. FITC-dextran permeability testing was performed as described in the assay protocol. Quantitative analysis of vascular permeability was performed using GraphPad Prism 5.0 (means ± SEM, n = 4). ***, $p < 0.001$ vs. Control; ###, $p < 0.001$, ##, $p < 0.01$, #, $p < 0.05$ vs. VEGF.

neolignan glycoside isolated from *Arum italicum*,[17] but the large coupling constant (J = 6.4 Hz) between C-7 and C-8 of **1**, compared to that of citrusin A ($J_{H\text{-}7/H\text{-}8}$ = 4.3 Hz) indicated a relative *threo*-configuration of the 1-phenyl-2-aryloxypropane-1,3-diol moiety in **1**.[17,18] This was confirmed by the observation of cross-peaks between H-8 and H-2/H-6, and H-8 and H-7 in the NOESY spectrum. The absolute configuration at C-7 and C-8 was determined to be 7*R* and 8*R* from the circular dichroism (CD) spectrum of **1** showing a negative Cotton effect in the region 220–250 nm, compared with those of reported analogs.[17,19,20] Hence, the structure of **1** was established as (7*R*,8*R*)-1-(4-*O*-β-D-glucopyranosyl-3-methoxyphenyl)-2-{2-methoxy-4-[1-(*E*)-propene-3-ol]-phenoxyl}-propane-1,3-diol.

The isolated compounds (**1**–**4**) were subjected to an *in vitro* bioassay to evaluate their effects on VEGF-induced vascular permeability in HRECs. Treatment of HRECs with **1**–**4** resulted in significant inhibition of VEGF-induced vascular permeability (Fig. 3), and no cytotoxicity was observed at the concentration used in this study. Of the compounds tested, compound **1** reduced the VEGF-induced vascular permeability most effectively by about 31.5% at 10 μM compared to the VEGF-treated control group. As cell migration is also essential for angiogenesis by endothelial cells,[21] we investigated the inhibitory effects of **1**–**4** on the chemotactic motility of endothelial cells by means of a wound-healing migration assay. As shown in Fig. 4, HREC migration induced by VEGF was significantly reduced by treatment with 10 μM **1** or **2** by about 56.4% and 53.6%, respectively, compared to the VEGF-treated control group.

The zebrafish is a vertebrate system and has been used extensively for drug screening and as a model of angiogenesis.[22] Thus, the effects of **1**–**4** on dorsal longitudinal anastomotic vessel (DLAV) development were assessed using *flk:EGFP* transgenic zebrafish embryos. We first examined the toxic effects of **1**–**4** on zebrafish; the results indicated no cytotoxicity for any of the test compounds at up to 80 μM (data not shown). To evaluate the effects of **1**–**4** on the DLAV formation, *flk:EGFP* transgenic zebrafish embryos were treated with DMSO (0.1%) or 80 μM **1**–**4**. As shown in Fig. 5, groups treated with **1** and **2** at 80 μM showed mild reductions of the DLAV formation by about 68.5% and 61.3%, respectively, compared with the 0.1% DMSO

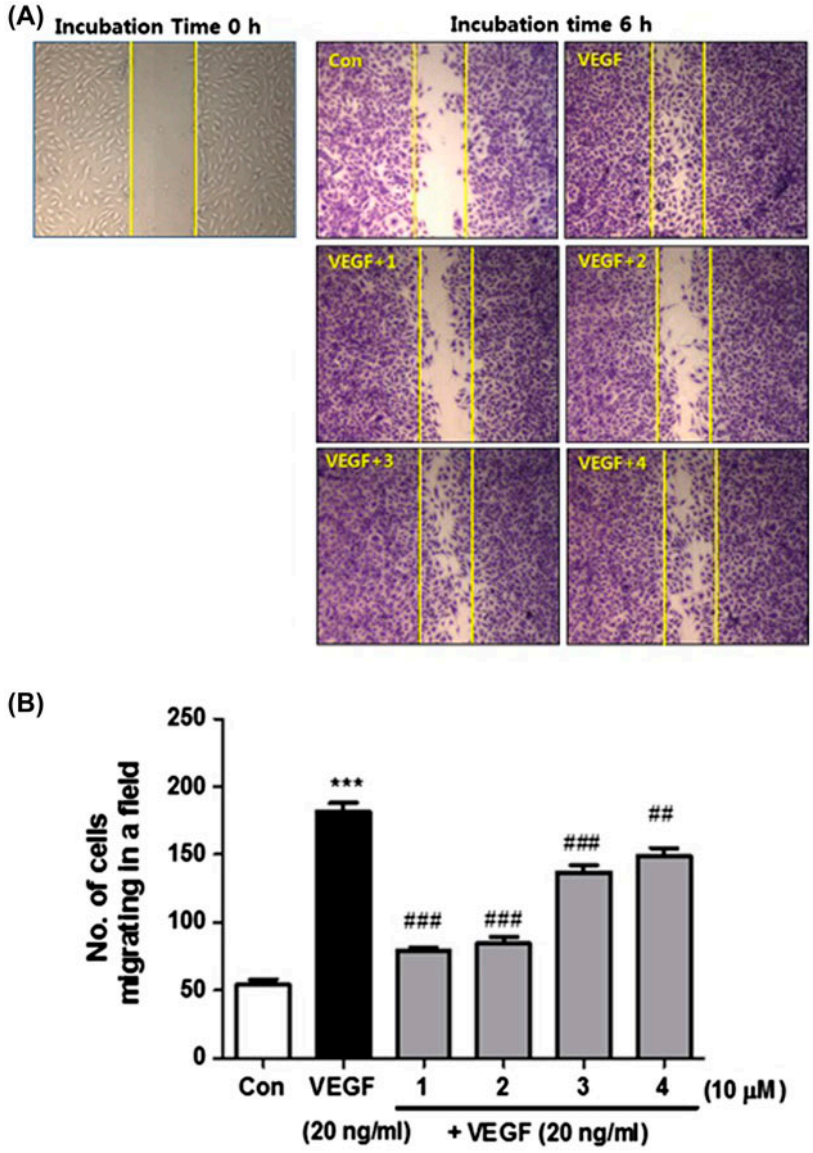

Fig. 4. Inhibitory effects of compounds **1**–**4** from *B. hancei* on VEGF-induced migration in HRECs.

Notes: HRECs were incubated in the presence of VEGF (20 ng/mL) and **1**–**4** (each 10 μM) for 6 h. The responses of HRECs to VEGF were determined using a scratch wound-healing assay. (A) Representative images before and after generation of the scratch are shown. (B) Quantitative analysis of cell migration was performed using GraphPad Prism 5.0 (means ± SEM, $n = 4$). ***, $p < 0.001$ vs. control; ###, $p < 0.001$, ##, $p < 0.01$ vs. VEGF.

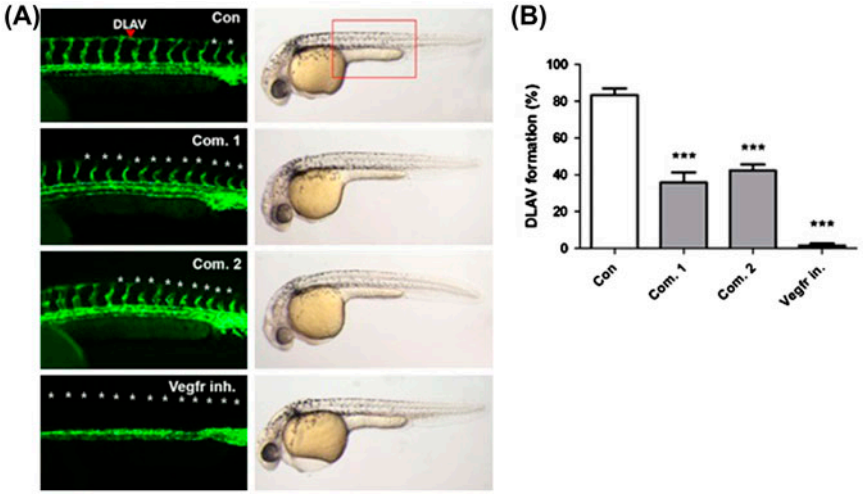

Fig. 5. Inhibitory effects of compounds **1** and **2** on DLAV formation in zebrafish embryos.

Notes: *flk*:EGFP transgenic zebrafish embryos were incubated in the presence of **1** or **2** (each 80 μM) or VEGFR inhibitor (1 μM) at 11 hpf, and gross morphological changes were examined. (A) Overall morphology and formation of the trunk vasculature. (B) Quantitative analysis of DLAV growth phenotypes was performed using GraphPad Prism 5.0 (means ± SEM, n = 8–10 embryos per each group). ***, $p < 0.001$ vs. control.

control group. The positive control, VEGFR inhibitor, induced serious defects in DLAV formation at 1 μM.

The present study aimed to identify effective antiangiogenic agents from the stems and leaves of *B. hancei* and resulted in the isolation of four lignans (**1**–**4**), including one new compound (**1**). This is the first report of the occurrence of lignans from *B. hancei*. These isolates (**1**–**4**) showed considerable inhibitory effects on VEGF-induced vascular permeability and migration of HRECs. Furthermore, we found that **1** and **2** reduced DLAV formation *in vivo* in a zebrafish model. Further studies are needed to better understand the specific mechanism(s) involved in the antiangiogenic effects of these compounds.

Funding

This research was supported by a grant [K14040] from the Korea Institute of Oriental Medicine. The NMR experiment was performed by the Korea Basic Science Institute (KBSI).

References

[1] He ZD, Wang DZ, Yang CR. Phenylpropanoid glycosides from *Brandisia hancei*. Acta Bot. Yunnanica. 1990;12:439–446.

[2] He ZD, Yang CR. Brandioside, a phenylpropanoid glycoside from *Brandisia hancei*. Phytochemistry. 1991;30:701–702.

[3] Kong LD, Wolfender JL, Cheng CH, Hostettmann K, Tan RX. Xanthine oxidase inhibitors from *Brandisia hancei*. Planta Med. 1999;65:744–746.

[4] He ZD, Huang Y, Yao X, Lau CW, Law WI, Chen ZY. Purification of phenylethanoids from *Brandisia hancei* and the antiproliferative effects on aortic smooth muscle. Planta Med. 2001;67:520–522.

[5] Zhou YC, Zheng RL. Phenolic compounds and an analog as superoxide anion scavengers and antioxidants. Biochem. Pharmacol. 1991;42:1177–1179.

[6] Murai M, Tamayama Y, Nishibe S. Phenylethanoids in the herb of *Plantago lanceolata* and inhibitory effect on arachidonic acid-induced mouse ear edema. Planta Med. 1995;61:479–480.

[7] Pettit GR, Numata A, Takemura T, Ode RH, Narula AS, Schmidt JM, Cragg GM, Pase CP. Antineoplastic agents, 107. Isolation of acteoside and isoacteoside from *Castilleja linariaefolia*. J. Nat. Prod. 1990;53:456–458.

[8] Xiong Q, Hase K, Tezuka Y, Tani T, Namba T, Kadota S. Hepatoprotective activity of phenylethanoids from *Cistanche deserticola*. Planta Med. 1998;64:120–125.

[9] Hayashi K, Nagamatsu T, Ito M, Hattori T, Suzuki Y. Acteoside, a component of *Stachys sieboldii* MIQ, may be a promising antinephritic agent (2): effect of acteoside on leukocyte accumulation in the glomeruli of nephritic rats. Jpn. J. Pharmacol. 1994;66:47–52.

[10] Pennacchio M, Alexander E, Ghisalberti EL, Richmond GS. Cardioactive effects of *Eremophila alternifolia* extracts. J. Ethnopharmacol. 1995;47:91–95.

[11] Didry N, Seidel V, Dubreuil L, Tillequin F, Bailleul F. Isolation and antibacterial activity of phenylpropanoid derivatives from *Ballota nigra*. J. Ethnopharmacol. 1999;67:197–202.

[12] Binu S, Soumya SJ, Sudhakaran PR. Metabolite control of angiogenesis: angiogenic effect of citrate. J. Physiol. Biochem. 2013;69:383–395.

[13] Dvorak HF, Brown LF, Detmar M, Dvorak AM. Vascular permeability factor/vascular endothelial growth factor, microvascular hyperpermeability, and angiogenesis. Am. J. Pathol. 1995; 146:1029–1039.

[14] Ferrara N, Davis-Smyth T. The biology of vascular endothelial growth factor. Endocr. Rev. 1997;18:4–25.

[15] Kim YS, Jung SH, Jung DH, Choi SJ, Lee YR, Kim JS. Gas6 stimulates angiogenesis of human retinal endothelial cells and of zebrafish embryos via ERK1/2 signaling. PLoS One. 2014;9: e83901.

[16] Achenbach H, Löwel M, Waibel R, Gupta M, Solis P. New lignan glucosides from *Stemmadenia minima*. Planta Med. 1992;58:270–272.

[17] Greca MD, Molinaro A, Monaco P, Previtera L. Neolignans from *Arum italicum*. Phytochemistry. 1994;35:777–779.

[18] Green TP, Galinis DL, Wiemer DF. Three neolignans from the roots of *Piper capense*. Phytochemistry. 1991;30:1649–1652.

[19] Fang JM, Lee CK, Cheng YS. Lignans from leaves of *Juniperus chinensis*. Phytochemistry. 1992;31:3659–3661.

[20] da Silva MS, Barbosa-Filho JM, Yoshida M, Gottlieb OR. Benzodioxane and β-aryloxy-arylpropane type neolignans from *Licaria chrysophylla*. Phytochemistry. 1989;28:3477–3482.

[21] Shibuya M. Vascular endothelial growth factor (VEGF)-Receptor2: its biological functions, major signaling pathway, and specific ligand VEGF-E. Endothelium. 2006;13:63–69.

[22] Serbedzija GN, Flynn E, Willett CE. Zebrafish angiogenesis: a new model for drug screening. Angiogenesis. 1999;3:353–359.